HAIT Journal of Science and Engineering B, Volume 2, Issues 5-6, pp. 625-637

Analysis and design of discrete sliding mode control for a nonresonant electronic ballast

René Osorio*, Mario Ponce, Marco Antonio Oliver,
Victor Hugo Olivares, and Mario Juárez

Electronic Engineering Department
National Center of Research and Technological Development (CENIDET)
Cuernavaca 62431, Morelos, Mexico
**Corresponding author: reneosorios@yahoo.com*

Received 1 March 2005, accepted 9 October 2005

Abstract

Analysis and design of a dimming control based on the Discrete Sliding Mode Control (DSMC) strategy for electronic ballast (without resonant tank) is presented. To avoid the acoustic resonance phenomenon, the proposed scheme feeds the lamp with low frequency square waves, and then, to stabilize the lamp current, a dc-dc converter with a closed-loop control stage is included. For this purpose, a buck converter with DSMC control is used. A fast response and good reference pursuit is obtained, avoiding the lamp turning off or the lamp destruction when the dimming control is implemented. A reduction in electronic elements is achieved and the reliability of the overall system is incremented with the DSMC compared to the analog Sliding Mode Control strategy. The analysis includes the conditions related to the existence of a sliding surface and the stability conditions. The simulations are made with a nonlinear dynamic lamp model. Analysis, simulation and experimental results of the proposed electronic ballast, and the control stage are presented.

Keywords: Electronic ballast, acoustic resonances, Discrete Sliding Mode Control, square waveforms, buck converter, continuous conduction mode, dimming.

1 Introduction

The acoustic resonance phenomenon in High Intensity Discharge (HID) lamps is a consequence of pressure waves in the gas inside the lamp. This phenomenon is caused by the lamp power modulation. The arc discharge is deformed by these pressure waves. Heating spots are generated when the glass bladder is reached by the arc, and generally these spots get broken [1].

One of the most reliable solutions for the elimination of the acoustic resonance phenomenon in HID lamps consists in feeding the lamp with square waveforms to reach a constant power. Most of the electronic ballasts that feed the lamps with square waveforms require a closed loop control stage to stabilize the lamp current [2,3].

Generally, when the HID lamps are fed with sinusoidal waveforms, the discharge arc in HID lamps is extinguished if the power inferior limit is reached (approximately 50% of the nominal power) [4]. Therefore, to avoid the arc extinction, it is important that the dimming control of the electronic ballast has a good reference tracking. Additionally, it is important to have a good dynamic response in illuminating systems where voltage variations or load changes are likely to occur.

Good dynamic response, stability, and regulation from voltage variations, are sought with the sliding mode control [5-6]. The HID lamp current is unstable when the lamp is fed with a voltage source, an example is a variable structure dc-dc converter working in continuous conduction mode (CCM). The control will drive the system to the balance point [5-6].

An igniter is needed when the HID lamps are fed with square waves. A proposed igniter is based on a resonant network; this network works only for 40μs-60μs in a high resonant frequency. Additionally, the semiconductor losses and the size of the passive elements are reduced.

An electronic ballast is presented in [7], feeding the HID lamp with low frequency square wave forms. The feedback control is designed with a nonlinear sliding control. The control stage is implemented in analog form, and then many electronic elements (1 operational amplifier, 1 high speed comparator, 2 logic circuits, 13 resistors, 1 microcontroller) are needed.

This work proposes to use a Discrete Sliding Mode Control for a non-resonant ballast. The following advantages are achieved against the Analog Sliding Mode Control [8]:

- reduction in the number of electronic components,
- possibility of generating adaptive control to feed different lamps with the same electronic ballast,

- flexibility in the sliding surface creation,
- the same control strategy is useful to different converters with minimum adjustment,
- possibility of integrating advanced functions into the control algorithm, like digital compensators, etc.

The above advantages are in addition to those introduced by the sliding mode control.

The simulations of the electronic ballast with the nonlinear dynamic lamp model [9] were made in Simulink (SimPowerSystem and DSP libraries).

This paper is organized as follows. An analysis of the power stage of selected ballasts is made in Section 2. In Section 3 an analysis of the control stage is made. An analysis of lamp model is made in Section 4. In Section 5, simulations and experimental results are presented, and finally the conclusions are given.

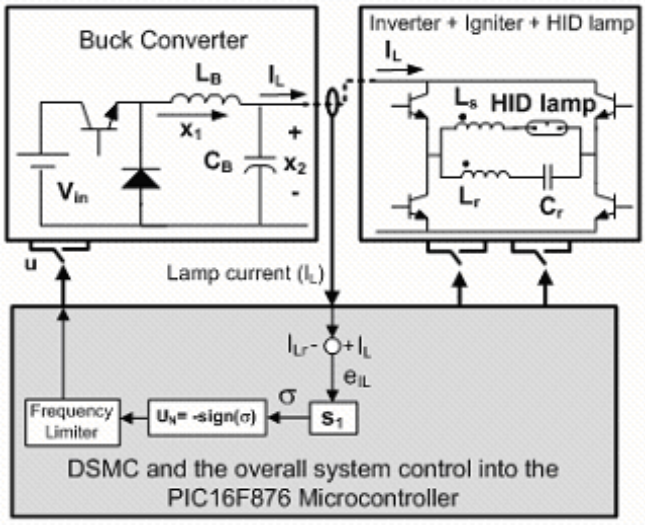

Figure 1: Block diagram of the selected topology with a nonlinear control stage.

2 Power stage

The block diagram of the selected ballast is shown in Fig. 1. A buck converter is operating in CCM. This converter stabilizes the arc discharge and

feeds the inverter. A dc bus is given by the dc-dc converter that integrates a power factor correction.

To avoid the acoustic resonance, the inverter feeds the HID lamp (70W metal Halide) with low frequency square waveforms (400Hz, avoiding the effects of parasitic elements).

The igniter is conformed by the resonant network (L_rC_r) in series configuration. L_r is coupled to L_s (autotransformer configuration). High voltages (4.5kV peak) can be reached with this configuration assuring the lamp ignition. The ignition sequence takes 40μs-60μs (4 or 6 pulses of 100 kHz). The operating frequency of the inverter changes to 400Hz when the lamp ignition is reached. Therefore, at this frequency, the inductor impedance is very low (short circuit) and the capacitor impedance is very high (open circuit), so that both impedances can be ignored.

3 Control stage

For DSMC design, the following steps must be developed [8, 10]: system modeling, sliding surface definition, control law, existence and convergence conditions of DSMC.

3.1 System modeling

The power stage, Fig. 2a, can be simplified by the following means. The influence of the igniter on the ballast in a stable state is worthless, Fig. 2b. The inverter current demanded from the buck converter is constant and can be eliminated, Fig. 2c. Finally, the semiconductors can be substituted by ideal switches, and the lamp is considered in a stable state as a constant resistance only for the controller parameters calculations, Fig. 2d. In the simulations, the lamp model proposed in [8, 11] is considered.

The resultant system in the matrix form considering the position of the switch u_1 (1 and -1) is:

$$\begin{pmatrix} \dot{x}_1 \\ \dot{x}_2 \end{pmatrix} = \begin{pmatrix} 0 & -\frac{1}{L_B} \\ \frac{1}{C_B} & -\frac{1}{C_B R} \end{pmatrix} \begin{pmatrix} x_1 \\ x_2 \end{pmatrix} + \begin{pmatrix} \frac{V_{in}}{2L_B} \\ 0 \end{pmatrix} u + \begin{pmatrix} \frac{V_{in}}{2L_B} \\ 0 \end{pmatrix} \quad (1)$$

or

$$\dot{X} = AX + BU + B \quad (2)$$

where x_1 is the L_B inductor current, x_2 is the C_B capacitor voltage.

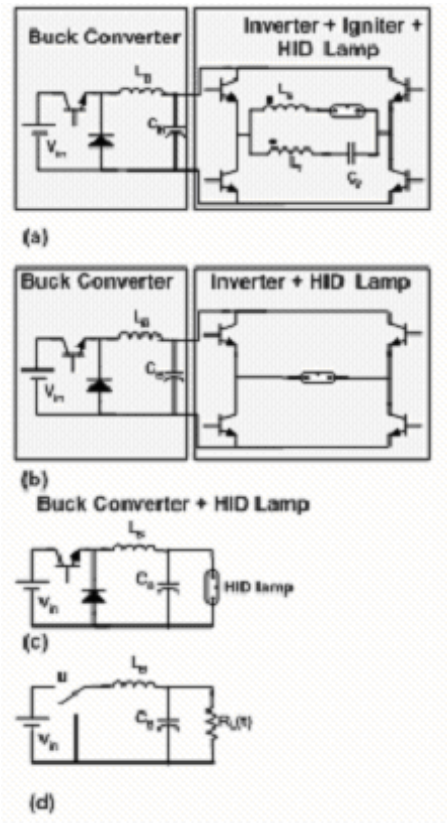

Figure 2: Ballast simplifications: (a) complete power stage, (b) without igniter, (c) without inverter, (d) using ideal switch and considering the lamp as a resistance.

For $L_B = 5\text{mH}$, $C_B = 1\mu\text{F}$, $R = 115\Omega$, $V_{in} = 180\text{V}$:

$$\begin{pmatrix} \dot{x}_1 \\ \dot{x}_2 \end{pmatrix} = 1e6 \begin{pmatrix} 0 & -0.0002 \\ 1 & -0.0087 \end{pmatrix} \begin{pmatrix} x_1 \\ x_2 \end{pmatrix} + \begin{pmatrix} 18e3 \\ 0 \end{pmatrix} u + \begin{pmatrix} 18e3 \\ 0 \end{pmatrix}. \quad (3)$$

The discrete system using a zero-order hold, with a sampling period of 16μs becomes:

$$\begin{pmatrix} x_1(n+1) \\ x_2(n+1) \end{pmatrix} = \begin{pmatrix} 0.9757 & \text{- } 0.002962 \\ 14.81 & 0.8469 \end{pmatrix} \begin{pmatrix} x_1(n) \\ x_2(n) \end{pmatrix} + \\ + \begin{pmatrix} 0.5713 \\ 2.1915 \end{pmatrix} u(n) + \begin{pmatrix} 0.5713 \\ 2.1915 \end{pmatrix}. \quad (4)$$

The PIC16F876 microcontroller from the Microchip Company was used.

3.2 The sliding surface

The continuous-sliding surface proposed in [12] is a linear combination of the lamp current (I_L) and the reference current (I_{Lr}) , Fig. 1:

$$\sigma = s_1 \left[I_L - I_{Lr} \right] \tag{5}$$

where s_1 is a control parameter.

In other notations,

$$\sigma = \left[\begin{array}{cc} s_2 & s_3 \end{array} \right] \left[\begin{array}{c} x_1 - x_{1r} \\ \frac{dx_2}{dt} - x_{2r} \end{array} \right] \tag{6}$$

where

$$s_2 = s_{1,} \tag{7}$$

$$s_3 = s_1 C_B, \tag{8}$$

x_{1r} and x_{2r} are the reference currents.

The discrete-sliding surface related to equation (6) is:

$$\sigma \left(n \right) = s_1 \left[I_L \left(n \right) - I_{Lr} \left(n \right) \right] = \left[\begin{array}{cc} s_2 & s_3 \end{array} \right] \left[\begin{array}{c} x_1 \left(n \right) - x_{1r} \\ \frac{x_2(n+1) - x_2(n)}{T} - x_{2r} \end{array} \right]. \tag{9}$$

Due to the operational amplifiers causing dc bus limitations, the s_1 experimental value is practically chosen in the (1, 10) interval, then the maxim value of s_3 is:

$$s_3 = s_1 C_B = 10e - 6 \ll s_2. \tag{10}$$

This implies to:

$$\sigma \left(n \right) \cong s_1 \left[x_1 \left(n \right) - x_{1r} \right] \tag{11}$$

where s_1, s_2, s_3 are the controller parameters, I_L is the current lamp, X is the state variables, I_{Lr}, X_r are the references.

The control law proposed is: $u = u_{eq} + u_N$ where u_{eq} is the equivalent control, $u_N = -\text{sgn}(\sigma)$.

3.3 The control law

The law is [10]:

$$u \left(n \right) = u_{eq} \left(n \right) + u_N \left(n \right) \tag{12}$$

where $u_N \left(n \right) = -\text{sgn} \left(\sigma \left(n \right) \right)$ is the implemented control, $U_{eq}(n)$ is the equivalent control.

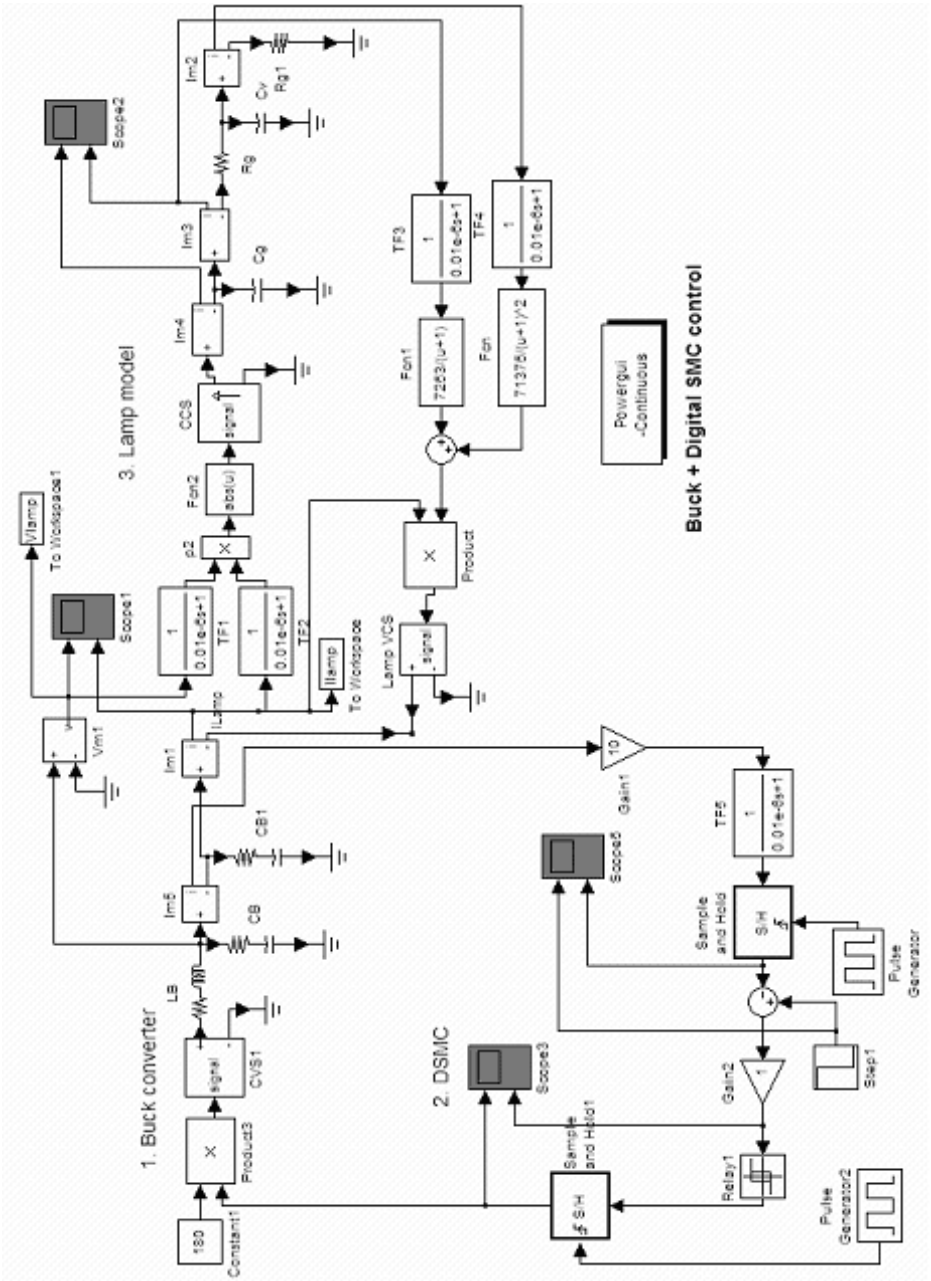

Figure 3: Simulated scheme in Simulink.

$U_{eq}(n)$ in the equivalent control law is used for the purposes of analysis, which implies a guarantee of the existence condition only locally.

The implemented control ($U_N(n)$) does not include the equivalent control.

3.4 The existence and convergence conditions of DSMC

Equations (13) and (14) describe the existence of DSMC [10]:

$$(\sigma(n+1)+\sigma(n))\,\mathrm{sign}(\sigma(n)) \geq 0, \text{ convergence condition,} \tag{13}$$

$$(\sigma(n+1)-\sigma(n))\,\mathrm{sign}(\sigma(n)) < 0, \text{ sliding condition.} \tag{14}$$

From experimental results, the lamp always ignites from the values: $x_1(n)$ = 3A (maximum value), $x_2(n)$= 20V, x_{1r} = 0.777A, and σ>0 when u_n = -1:

$$4.31 s_1 \geq 0, \text{ convergence condition,} \tag{15}$$

$$-0.78 s_1 < 0, \text{ sliding condition,} \tag{16}$$

$x_1(n)$ = 0.35A (minimum value), $x_2(n)$= 115V, x_{1r} = 0.777A, and σ<0 when u_n = 1:

$$0.06 s_1 \geq 0, \text{ convergence condition,} \tag{17}$$

$$-0.13 s_1 < 0, \text{ sliding condition.} \tag{18}$$

Then s_1 must be positive to satisfy equations (15) to (18).

4 Simulation and experimental results

The electronic ballast was designed with the following parameters: P_o = 70W, V_{in} =180V, V_C = 90V, I_L = 0.777A, L = 5mH, C = 1μF, CDM70W830PH lamp, s_1 = 1. The C and L values were designed according to current and voltage ripples.

In Fig. 3, the simulated circuit (buck converter, DSMC and lamp model) is shown. Simulation results of the electronic ballast with DSMC control are shown in Figs. 4 and 5. In Fig. 4, the current demanded and the output voltage of the buck converter are shown. In Fig. 5, a dimming test (from 100% to 50%) is shown; this dimming is made with a change in the reference current. The demanded current and the output voltage to the buck converter are shown. As it can be observed, a good dynamic response is obtained. In these figures the effect of death times is shown.

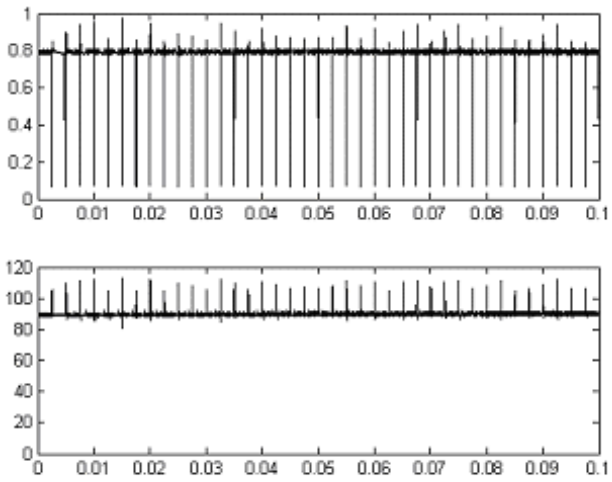

Figure 4: Waveforms for nominal power (70 W): (a) typical topology: current demanded (top) and output voltage of a buck converter; (b) compact topology: lamp current (top) and lamp voltage (bottom).

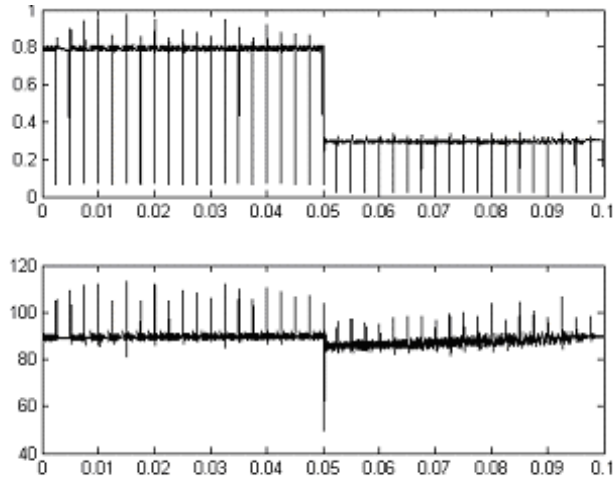

Figure 5: Dimming test (from 100% to 50%), (a) typical topology: current demanded (top) and output voltage of aa buck converter; (b) compact topology: lamp current (top) and lamp voltage (bottom).

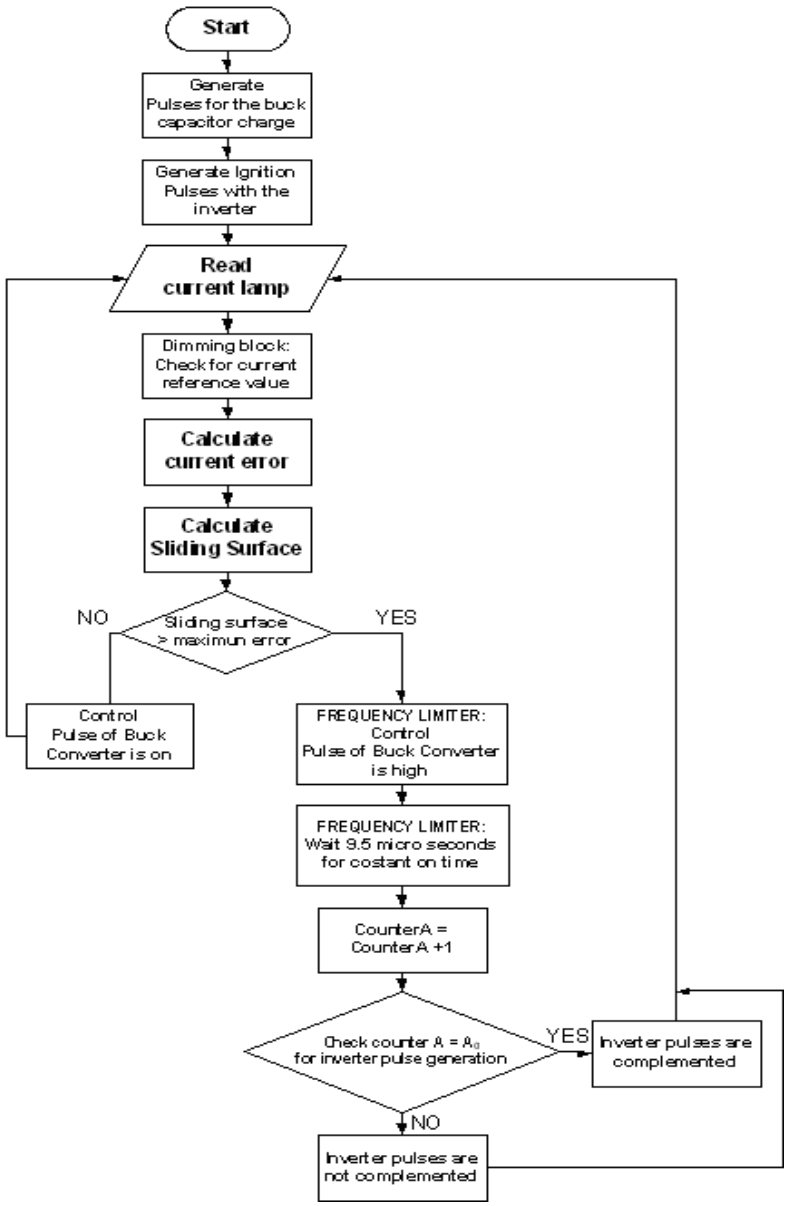

Figure 6: DSMC program flux diagram implemented in the PIC16F876 microcontroller.

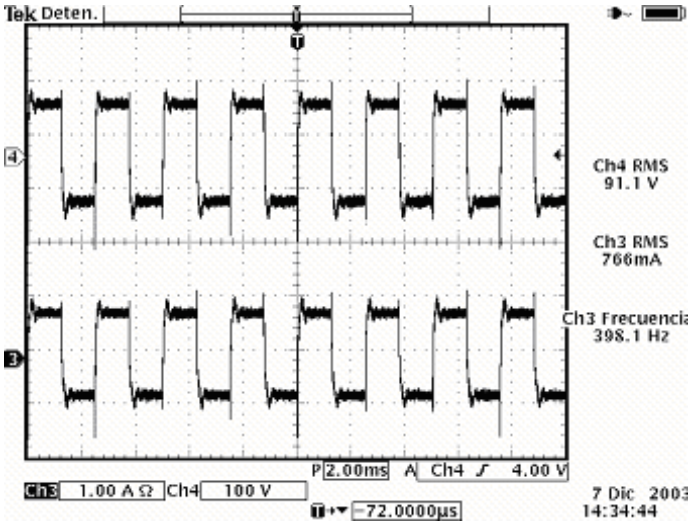

Figure 7: Experimental results. Top to bottom: lamp current and lamp voltage.

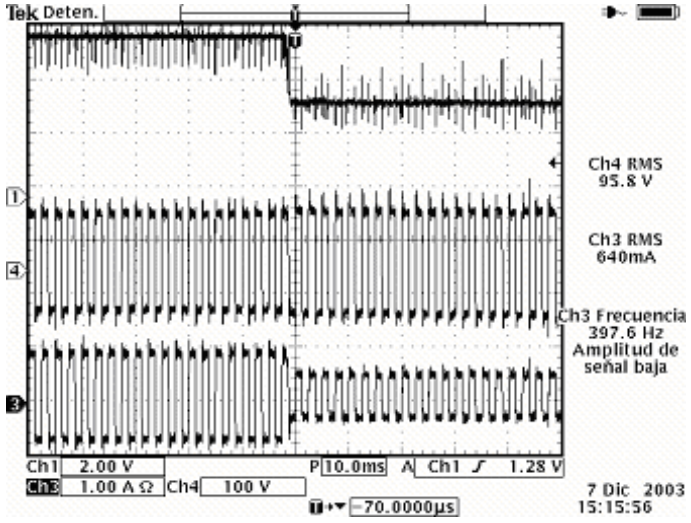

Figure 8: Experimental results, dimming test (from 100% to 50%). Top to bottom: lamp current and lamp voltage.

In Fig. 6, the DSMC program flux diagram is shown and in the Fig. 7 the diagram schematic stage control is shown. Experimental results of the electronic ballast with DSMC control are shown in Figs. 7 and 8. Fig. 7 presents the experimental results of the electronic ballast with a SMC control under steady state conditions. The reference current, lamp current and voltage are shown. In Fig. 8, a dimming test (from 100% to 50%) is shown; this dimming is made with a change in the reference current. The current demanded and the output voltage of the buck converter is shown. As it can be observed, a good dynamic response is obtained.

5 Conclusions

In this paper an analysis of a HID lamp under the action of a discrete sliding mode nonlinear control (SMC) is presented. To avoid the appearance of acoustic resonance, the power stage feeds the HID lamp with low frequency square waves. A good dynamic response in dimming test is obtained because the control strategy is efficient. Also, the nonlinearity is considered in the buck model and the lamp model. This is an other advantage of the nonlinear control strategy over the classic control strategy, because when a linearization model is obtained, the analysis is limited to a region close to the operation point.

The dynamic nonlinear Pspice lamp model implementation in Simulink was also shown.

The experimental results had shown a good behavior of the selected electronic ballast with a nonlinear control stage (SMC). Square waves are obtained with this topology and hence, the acoustic resonance phenomenon is eliminated.

This work was supported by the National Council of Science and Technology (CONACYT) and the National Council for Technological Education (COSNET), Mexico.

References

[1] J.J. Groot and J.A.J.M. Van Vliet, *The High-Pressure Sodium Lamp* (Editorial Macmillan Education, 1986).

[2] E. Deng, *Negative Incremental Impedance of Fluorescent Lamp*, Ph.D. Thesis, California Institute of Technology, Pasadena, 1995.

[3] E. Deng and S. Cuk, Applied Power Electronic Conference, APEC'97, Atlanta, Ga, USA, p.1050 (1997).

[4] J. Correa, M. Ponce, J. Arau, and J.M. Alonso, Industry Applications Conference, IAS'02, Pittsburgh, Pa, USA, p.1467 (2002).

[5] V.I. Utkin, *Sliding Modes and Their Application in Variable Structure Systems* (Mir, Moscow, 1974).

[6] V. Utkin, Trans. Automatic Control 1977, 212 (1977).

[7] M. Ponce, A. Lopez, J. Correa, J. Arau, and J.M. Alonso, Applied Power Electronics Conference and Exposition, APEC'01, Anaheim, Ca, USA, v.**2**, p.658 (2001).

[8] R. Orosco and N. Vazquez, VII IEEE International Power Electronics Congress, CIEP'2000, Acapulco, Mexico, p.231 (2000).

[9] R. Osorio, M. Ponce, and M.A. Oliver, 35th Annual IEEE Power Electronics Specialists Conference, PESC'04 (2004).

[10] S. Sarpturk, Y. Istefanopulos, and O. Kaynak, IEEE Trans. on Automatic Control **32**, 930 (1987).

[11] R. Osorio, M. Ponce, and M.A. Oliver, Applied Power Electronic Conference, APEC'04, Aachen, Germany (2004).

[12] R. Osorio, M. Ponce, and M.A. Oliver, Congreso Latinoamericano de Control Automático, CLCA'04 (2004).